Self-organized exotic lattices with ultracold gases

O. Dutta[1] and A. Przysiężna[2,3], and M. Lewenstein[1,4]
[1] *ICFO —Institut de Ciencies Fotoniques, Av. Carl Friedrich Gauss, num. 3, 08860 Castelldefels (Barcelona), Spain*
[2] *Institute of Theoretical Physics and Astrophysics, University of Gdańsk, Wita Stwosza 57, 80-952 Gdańsk, Poland*
[3] *National Quantum Information Centre of Gdańsk, Andersa 27, 81-824 Sopot, Poland*
[4] *ICREA – Instituciø Catalana de Recerca i Estudis Avançats, Lluis Companys 23, E-08010 Barcelona, Spain*
(Dated: February 12, 2013)

We study an ultracold Fermi-Fermi mixture of strongly attractive atoms trapped in a square lattice. We show that the interaction-induced multi-band nature of such system can change the inherent structure of the original lattice. The dynamically generated lattice resembles geometrically a Lieb lattice with interaction-driven topological insulator phases.

PACS numbers: 67.85.Lm, 03.75.Lm, 73.43.-f

Currently, there is a great interest in the investigation of topologically insulating states in solid-state physics [1, 2] due to their potential applications in spintronics, topologically protected quantum computing [3], and apintomics [4]. In this regard, due to the enormous control and possibility of quantum engineering [4], systems of ultracold gases trapped in optical lattices provide promising avenues to follow. One such avenue concerns optical creation of frustrated lattice geometries [5–7] with tunable long-range hopping amplitudes, which can induce a variety of exotic phenomena like topological insulators, ferromagnetism etc. [8–15]. Recently, other ways to induce topologically insulating states such as quantum anomalous Hall states (QAH) and quantum spin Hall states (QSH) were investigated. Particularly interesting is the dynamical creation of interaction-driven topological insulators in lattices with quadratic band-crossing points ($QBCP$) [16–19]. The most promising lattice structure to have $QBCP$ within the Brillouin zone is a Lieb lattice. In [20, 21], the authors have proposed to create such geometry by optical means which, however, is not easy to realize experimentally. In the spirit of dynamical generation of topological states, we propose in this letter how to create such non-trivial lattice structures due to self-organization of the ultracold gases. Furthermore we show that in our system one can study the appearance of interaction-driven QAH and/or QSH states.

We consider a mixture of two-species ultracold fermionic atoms trapped in an optical lattice potential $V_{\sigma,\text{latt}} = V_{\sigma,x}\sin^2(\pi x/a) + V_{\sigma,y}\sin^2(\pi y/a) + V_{\sigma,z}\sin^2(\pi z/a)$, where $\sigma = \uparrow,\downarrow$ denotes the two species and $V_{\sigma,x(y)(z)}$ are the corresponding lattice depths for σ-fermions along the x, y, z direction respectively. The corresponding recoil energies are $E_{\text{R}\sigma} = \pi^2\hbar^2/2m_\sigma a^2$, where m_σ denotes the mass of the σ-fermion. The filling of the σ-fermion is given by n_σ. For simplicity we consider the case in which fermionic masses are equal, i.e $m_\downarrow = m_\uparrow$. Subsequently, we define the recoil energy $E_\text{R} = E_{\text{R}\sigma}$. For the two-dimensional ($2D$) geometry we choose $V_0 = V_{\downarrow,x} = V_{\downarrow,y}$, $V_1 = V_{\downarrow,z} = V_{\uparrow,x(y)(z)}$, and $V_1 \gg V_0$, which means that the $\downarrow$-fermions can effectively move in the $x-y$ plane with the z motion freezed. The atoms interact with each other via s-wave scattering with strength a_s. Within the lowest-band, we can write the corresponding attractive Fermi-Hubbard model as $H_1 = -\sum_{\langle\mathbf{i},\mathbf{j}\rangle,\sigma} J_{0\sigma}\hat{s}^\dagger_{\sigma\mathbf{i}}\hat{s}_{\sigma\mathbf{j}} - |U|/2\sum_{\mathbf{i},\sigma\neq\sigma'}\hat{n}_{\mathbf{i}\sigma}\hat{n}_{\mathbf{i}\sigma'}$. Here $\hat{s}^\dagger_{\sigma,\mathbf{i}}$ and $\hat{s}_{\sigma,\mathbf{i}}$ are the creation and annihilation operators for the σ-fermions in the s-band at site $\mathbf{i} = (i_x, i_y)$ with density $\hat{n}_{\sigma,\mathbf{i}}$ and the contact interaction $|U| = 4\pi\hbar^2|a_s|/m_\text{r}$ with m_r being the reduced mass. $J_{0\sigma}$ is the tunneling strength of the σ-fermions in the s-band and $\langle\mathbf{i},\mathbf{j}\rangle$ denotes nearest neighbours in the square lattice. As the $\uparrow$-fermions move in a deeper lattice ($J_{0\downarrow} \gg J_{0\uparrow}$), consequently we neglect the tunneling of the $\uparrow$-particles. In this paper we look into the spin-imbalanced situation with $n_\downarrow > n_\uparrow$ with the excess $\downarrow$-fermions (denoted below by s-fermion) filling $m = n_\downarrow - n_\uparrow$. In the regime of strong attractive interaction strength, $|U| \gg J_{0\downarrow}$, the $\uparrow$ and $\downarrow$-fermions will like to pair up to form composites with creation operator $\hat{b}^\dagger_\mathbf{i} = \hat{s}^\dagger_{\uparrow\mathbf{i}}\hat{s}^\dagger_{\downarrow\mathbf{i}}$ and density $\hat{n}^B_\mathbf{i}$ [22–24]. Such a pair can tunnel only due to second order processes which are practically negligible. We can rewrite the Hamiltonian for the composites and s-fermions as, $H_1 = -J_0\sum_{\langle\mathbf{i},\mathbf{j}\rangle}\hat{s}^\dagger_\mathbf{i}\hat{s}_\mathbf{j} - |U|\sum_\mathbf{i}\hat{n}^B_\mathbf{i}$, where we have removed the $\downarrow$ subscript as only the $\downarrow$-fermions are involved in the dynamics. Recently it has been noted that in the strong interaction regime, the standard Hubbard models have to be modified due to both intra- and inter-band effects [25–28]. To take these effects into account we write a minimal model for the excess $\downarrow$-fermions by including the occupation of the p-band and renormalization of the interaction. The inclusion of a p-band allows a $\downarrow$-fermion to occupy the same site as a composite. The single-particle tunneling Hamiltonian then reads, $H_\text{t} = -J_0\sum_{\langle\mathbf{ij}\rangle}\hat{s}^\dagger_\mathbf{i}\hat{s}_\mathbf{j} + J_1\sum_{\langle\mathbf{ij}\rangle_x}\hat{p}^\dagger_{x\mathbf{i}}\hat{p}_{x\mathbf{j}} + J_1\sum_{\langle\mathbf{ij}\rangle_y}\hat{p}^\dagger_{y\mathbf{i}}\hat{p}_{y\mathbf{j}} - J_0\sum_{\langle\mathbf{ij}\rangle_y}\hat{p}^\dagger_{x\mathbf{i}}\hat{p}_{x\mathbf{j}} - J_0\sum_{\langle\mathbf{ij}\rangle_x}\hat{p}^\dagger_{y\mathbf{i}}\hat{p}_{y\mathbf{j}}$, where $\hat{p}^\dagger_x, \hat{p}_x$ $(\hat{p}^\dagger_y, \hat{p}_y)$ are creation and annihilation operators of the $\downarrow$ particles in the $p_x(p_y)$-band. J_1 is the single-particle tunneling amplitude in the p-band, and $\langle\mathbf{ij}\rangle_{x(y)}$ denotes the nearest-neighbour sites along the $x(y)$-direction. Next we write

the interaction-induced tunneling terms in the p-band as:

$$H_{\rm T} = \sum_{\delta} \Bigg[J_{11} \sum_{\langle \mathbf{ij} \rangle_{\delta}} \hat{p}^{\dagger}_{\delta \mathbf{i}} (\hat{n}^{B}_{\mathbf{i}} + \hat{n}^{B}_{\mathbf{j}}) \hat{p}_{\delta \mathbf{j}} - J'_{11} \sum_{\langle \mathbf{ij} \rangle_{\delta'}} \hat{p}^{\dagger}_{\delta \mathbf{i}} (\hat{n}^{B}_{\mathbf{i}} + \hat{n}^{B}_{\mathbf{j}}) \hat{p}_{\delta \mathbf{j}} \Bigg], \quad (1)$$

where $\delta, \delta' = x, y$ with $\delta \neq \delta'$ and J_{11} denotes intra-band interaction-induced tunneling for $p_x(p_y)$-fermions along $x(y)$ directions, whereas J'_{11} denotes interaction-induced tunneling for $p_x(p_y)$-fermions along $y(x)$ directions. Such terms originate from the nearest-neighbour scattering due to interaction and give the most important contribution to the renormalization of intra-band tunneling [29]. The interaction induced term has another component which can mix the s- and p-bands and can be written as

$$H_{01} = J_{01} \sum_{\delta = x,y} \sum_{\langle \mathbf{ij} \rangle_{\delta}} \zeta_{i_{\delta}, j_{\delta}} \hat{p}^{\dagger}_{\delta \mathbf{i}} \hat{n}^{B}_{\mathbf{i}} \hat{s}_{\mathbf{j}} + h.c, \quad (2)$$

where J_{01} denotes the interaction induced inter-band tunneling and $\zeta_{i_{\delta}, j_{\delta}} = (-1)^{i_{\delta} - j_{\delta}}$ denotes the staggered nature of the $s-p$ tunneling matrix. Such hybridization between bands due to interaction induced tunneling is an important feature of the strongly interacting gases in optical lattices and usually has been neglected in the literature. Next we describe the on-site Hamiltonian for the excess $\downarrow$-fermions and the composites,

$$H_{\rm int} = -|U_2| \sum_{\mathbf{i}} \hat{n}^{B}_{i} - |U_3| \sum_{\mathbf{i}} \hat{n}^{B}_{\mathbf{i}} (\hat{n}_{x\mathbf{i}} + \hat{n}_{y\mathbf{i}}) - |\delta U_3| \sum_{\mathbf{i}} \hat{n}_{x\mathbf{i}} \hat{n}_{y\mathbf{i}} \hat{n}^{B}_{\mathbf{i}} + E_1 \sum_{\mathbf{i}} (\hat{n}^{p}_{x\mathbf{i}} + \hat{n}^{p}_{x\mathbf{i}}), \quad (3)$$

where $\hat{n}_{x(y)\mathbf{i}} = \hat{p}^{\dagger}_{x(y)\mathbf{i}} \hat{p}_{x(y)\mathbf{i}}$. The renormalized self-energy of the composite is given by U_2 and U_3 is the strength of the renormalized onsite interactions between a composite and a $\downarrow$-fermion in the p band at a site. The effective three-body interaction term $\delta U_3 = U_4 - 2U_3$ denotes the excess energy, where U_4 is the energy of a single site containing one composite and one $\downarrow$-fermion each in the p_x and p_y orbitals. In our problem we calculate the difference $U_3 - U_2$ and δU_3 within the second order perturbation which converges quickly with respect to band indices [30] and remains valid in the attractive interaction regime. We find that δU_3 is small compared to other parameters, so we neglect it at first. Here we like to comment that we derive all the tunneling and interaction parameters by writing them in terms of Wannier functions as described in the seminal paper [31].

The total Hamiltonian $H = H_{\rm T} + H_{01} + H_{\rm int}$ does not contain any tunneling of the composites, which makes the commutator $[\hat{n}^{B}_{\mathbf{i}}, H] = 0$. In such a case $n^{B}_{\mathbf{i}} = 0, 1$ becomes a good quantum number for the system. The ground state of the Hamiltonian H can be found by comparing the energies for different configurations of $n^{B}_{\mathbf{i}}$ over the entire lattice by solving the corresponding single particle Hamiltonian H. We have found the lowest energy configurations of the composites for various parameters by using simulated annealing method on a 8×8 lattice with periodic boundary condition. We like to point out here that due to the interaction-induced origin of tunneling terms in Eq.(1) and (2), their strengths and signs are defined by the various lattice depths and effective interaction strength $\alpha = a_s/a$. For half-filled composites ($n^{B} = 1/2$) the phase diagrams are shown in Fig.1. In Fig.1(a) we show the different phases as a function of m and the effective scattering length $\alpha = a_s/a$. Various phases of the composites as shown in Fig. 2 are: i) checkerboard structure with period one (*CH1*-the red region, shown in Fig.2b), ii) checkerboard structure with period 2 (*CH2*-the light-blue region), iii) stripe phase (the green region), iv) phase-separated state (the black region), and v) mixed phase characterized by absence of any periodic structure (the yellow region). The phase-separated state is characterized by the clustering of the composites to one region of the lattice, whereas in the stripe phase alternative chains of the lattice are occupied by the composites. The *CH2* and the stripe phase are only present in a small region of the phase space for very low filling of the excess $\downarrow$-fermions with discontinuous structural transitions. Here one should keep in mind that the total Hamiltonian H has similar feature to the celebrated Falicov-Kimball (FK) model where one can get a zoo of discontinuous structural phase transitions [32]. However, normal FK models do not possess the multi-orbital nature and density-dependent tunnel-

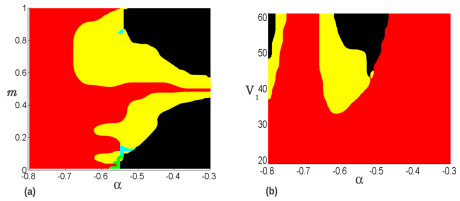

FIG. 1. (Colour online) (a) The phase diagram for the configurations of the composites as a function of normalized interaction strength $\alpha = a_s/a$ and excess $\downarrow$-fermion filling m for $n^{B} = 1/2$. The red coloured region denotes the period-1 checkerboard configuration for the composites. The black region denotes the phase-separated phase, the light-blue region denotes the period-2 checkerboard phase, the green region denotes the stripe phase and the yellow region contains mixed phase. The lattice parameters are $V_0 = 4E_{\rm R}, V_1 = 30E_{\rm R}$.(b) The phase diagram with fixed $m = 1/2$ and composite filling $n^{B} = 1/2$ for $V_0 = 4E_R$. The phases are depicted as a function of interaction strength α and lattice depth V_1.

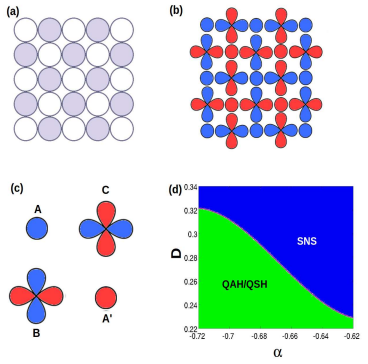

FIG. 2. (Colour online) (a) The figure shows the distribution of the composites in the *CH1* phase. The filled (empty) circles denotes presence(absence) of a composite. (b) The figure denotes the corresponding orbital degrees of freedom for the excess ↓-fermions. The coloured circle denotes the s-orbitals. The horizontal (vertical) coloured dumb-dell shapes denotes $p_x(p_y)$-orbitals. (c) Pictorial description of the basis states for the blue (red) lattice $\mathbf{A}, \mathbf{B}$ and $\mathbf{C}$ ($\mathbf{A}', \mathbf{B}$ and $\mathbf{C}$). (d) The ground state phase diagram corresponding to the Hamiltonian (5) as a function of dipolar strength D and contact interaction strength α for $V_0 = 4E_{\rm R}$, half-filled composites ($n^B = 1/2$) and excess ↓-fermion filling $m = 1/2$.

ing processes as present in our system. The mixed phase occurs in the region where the energy cost to occupy the p-orbital is small compared to other tunneling processes. Thus it is possible that the mixed phase is a disordered phase due to the composite density dependence on the tunneling processes. Such mixed phases have not been predicted before in FK like models. However one should be cautious about an assertion regarding the *CH2*, stripe and mixed phases in our paper, since they can be an effect of the finite size of the system. Subsequently apart from the *CH1* and the phase-separated state, we will not consider other structures in the remaining part of this paper. In Fig.1(b) we plot the phase diagram as a function of α and V_1 with the excess ↓-fermion density $m = 1/2$. The most interesting region is *CH1* thus let us mainly focus on it. The presence of *CH1* region can be qualitatively predicted when the $s-p$ tunneling strength J_{01} becomes comparable to the inter-band tunneling strengths, i.e $|J_{01}| \gtrapprox max\{|J_1 + J_{11}|, J_0\}$, specially for $m = 1/2$. The *CH1* phase of the composites is shown in Fig.2(a). The corresponding lattice structure seen by the excess ↓-fermions is shown in the right panel in Fig.2(b). The coloured circular sites denotes s-orbitals and the dumb-bell shaped sites denote p_x or p_y orbitals. Due to the directional nature of the inter-orbital tunneling J_{01} in Hamiltonian (2) and the absence of any on-site orbital mixing term in (3), the motion of the excess fermions can be divided into two sub-lattices shown by blue and red colour in Fig.2(b). Each of the red and blue sub-lattices have the structure of an exotic Lieb lattice. In Fig.2(c) we show the basis sites for the blue Lieb lattices denoted by $\mathbf{A}, \mathbf{B}$ and $\mathbf{C}$ ($\mathbf{A}', \mathbf{B}$ and $\mathbf{C}$ for the red Lieb lattice). The excess ↓-fermions moving in the blue sub-lattice are denoted by, $\Phi_1 = [\hat{s}_A, \hat{p}_{\rm yB}, \hat{p}_{\rm xC}]$ and the corresponding operators in the red sub-lattice are denoted by $\Phi_2 = [\hat{s}_{A'}, \hat{p}_{\rm xB}, \hat{p}_{\rm yC}]$. Their motion is governed by the Hamiltonian,

$$H = J_{01}\left[\sum_{\langle \mathbf{ij}\rangle_x} \zeta_{i_x,j_x}\hat{s}^\dagger_{\rm A\mathbf{i}}\hat{p}_{\rm xC\mathbf{j}} + \sum_{\langle \mathbf{ij}\rangle_y} \zeta_{i_y,j_y}\hat{s}^\dagger_{\rm A\mathbf{i}}\hat{p}_{\rm yB\mathbf{j}} + \sum_{\langle \mathbf{ij}\rangle_x} \zeta_{i_x,j_x}\hat{s}^\dagger_{\rm A'\mathbf{i}}\hat{p}_{\rm xB\mathbf{j}} + \sum_{\langle \mathbf{ij}\rangle_y} \zeta_{i_y,j_y}\hat{s}^\dagger_{\rm A'\mathbf{i}}\hat{p}_{\rm yC\mathbf{j}} + h.c\right]$$
$$+ \Delta \sum_{\mathbf{i},\tau=\mathbf{B},\mathbf{C}} (\hat{n}_{\tau\mathbf{i}} + \hat{n}_{\tau\mathbf{i}}) - |\delta U_3| \sum_{\mathbf{i},\tau=B,C} \hat{n}_{x\tau\mathbf{i}}\hat{n}_{y\tau\mathbf{i}}. \quad (4)$$

Here the first term inside the [.]-bracket in Eq.(4) is a reformulation of H_{01} in Eq(2). The second term refers to the energy cost of the p-orbital atoms occupying a site already taken by a composite, $\Delta = E_1 - |U_3| + |U_2|$. The third term describes effective onsite interactions between the red and blue fermions in the sites B and C. The single particle dispersion relation of Lieb lattice is given by $\epsilon_{\mathbf{k}} \in \{\Delta, \Delta/2 \pm \sqrt{(\Delta/2)^2 + 4J_{01}^2\left[\sin^2 k_x + \sin^2 k_y\right]}\}$, where momentum $\mathbf{k} = (k_x, k_y)$ belongs to reduced Brillouin zone $(\pi/2, \pi/2)$. The dispersion contains Quadratic Band-Crossing point(QBCP) for $\Delta \lesseqgtr 0$ with one of the dispersive bands touching the flat band at momentum $(0,0)$. At $\Delta = 0$, three bands touch each other at the momentum $(0,0)$ with the upper and lower band having linear dispersion for $k \ll 1$. For simplicity we consider only the case when $\Delta < 0$. Then we can write an effective two band Hamiltonian $H = d_0\mathcal{I} + d_z\sigma_z + d_x\sigma_x$, where $\sigma_{x(z)}$ are the Pauli matrices, $\mathcal{I}$ is the identity matrix, $d_0 = (J_{01}^2/\Delta)(\cos 2k_x + \cos 2k_y)$ and the vector $\vec{d} = (d_x, d_z) = (J_{01}^2/\Delta)(\cos 2k_x - \cos 2k_y, 4\sin k_x \sin k_y)$. In this limit, the particles occupy only the B, C sites of the lattice and the population in the A, A' sites is negligible. For excess fermion filling $m = 1/2$, the dispersive band is filled and the system becomes a band insulator. There is a topological index $W = \pm 2$ associated with the vector $\vec{d}$ which makes the QBCP topologically stable for non-interacting systems and the corresponding

Berry phase is given by $W\pi$. This shows that, due to interaction-induced tunneling, one can dynamically generate topologically protected exotic lattices from simple geometry. To the best of our knowledge, such proposals of dynamical generation of non-zero Berry phase from a topologically trivial non-frustrated lattice (square lattice in our case) have not been proposed before.

The dynamical realization of Lieb lattice opens up an alternative way to study the possibility of generating integer quantum Hall effects in such systems. One possible way is to induce effective spin-orbit coupling, which can be achieved by optical means [33] or by lattice-shaking [34]. Another promising way is to generate such coupling dynamically by including long-range interactions which can create *QAH* and *QSH* states [16, 17]. Such models are usually hard to implement in experimentally realizable system as one needs the on-site interactions to be of the same order of magnitude as the long-range part of the interaction [18]. To investigate such possibility in our system we add additional dipolar term for the excess $\downarrow$-fermions,

$$\begin{aligned} H_{\rm full} &= H + H_{\rm dd}, \\ H_{\rm dd} &= U_{\rm dd}\sum_{\mathbf{i},\tau}\hat{n}_{x\tau\mathbf{i}}\hat{n}_{y\tau\mathbf{i}} + \frac{U_{\rm xy}}{2}\sum_{\langle\langle\mathbf{i},\mathbf{j}\rangle\rangle,\tau\neq\tau'}\hat{n}_{x\tau\mathbf{i}}\hat{n}_{y\tau'\mathbf{j}} \\ &+ \frac{U_{\rm xx}}{2}\sum_{\langle\langle\mathbf{i},\mathbf{j}\rangle\rangle,\tau}[\hat{n}_{x\tau\mathbf{i}}\hat{n}_{x\tau\mathbf{j}} + \hat{n}_{y\tau\mathbf{i}}\hat{n}_{y\tau\mathbf{j}}], \end{aligned} \tag{5}$$

where $U_{\rm dd}$ is onsite dipolar interaction, $U_{\rm xy}$ is interaction between the particles in p_x and p_y-orbital in B and C sites respectively, and $U_{\rm xx}$ is next-nearest neighbour interaction between the particles in p_x and p_x-orbital (also between p_y and p_y orbital) in B and C sites. $\langle\langle\mathbf{i},\mathbf{j}\rangle\rangle$ denotes next-nearest neighbour p-orbital sites. We additionally introduce the dimensionless dipolar interaction strength $D = \mu_0\mu^2 m_\downarrow/2\hbar^2 a$, where μ is the magnetic dipole moment of the atoms and μ_0 is the vacuum permeability. In this unit, the dipole-dipole interaction has the form, $U_{\rm dd}(r) = D(1-3z^2/r^2)/r^3$, where r is the inter-particle distance. For experimental realization, the suitable candidates are fermionic ^{161}Dy which is experimentally available in quantum degenerate state [35], and possibly fermionic ^{167}Er [36]. Due to the strong attractive contact interaction $|U|$, the effect of dipolar terms on Δ is negligible. We also neglect the effective long-range repulsion between the composites which can further stabilize the *CH1* phase. Within weak-coupling limit we can define the mean-field parameters,

$$\begin{aligned} &\langle\hat{p}^\dagger_{xBi}\hat{p}_{yCj}\rangle = \langle\hat{p}^\dagger_{yBi}\hat{p}_{xCj}\rangle = i\chi_{\rm QAH}, \\ &\langle\hat{p}^\dagger_{xBi}\hat{p}_{yCj}\rangle = -\langle\hat{p}^\dagger_{yBi}\hat{p}_{xCj}\rangle = i\chi_{\rm QSH}, \\ &\langle\hat{n}_{xBi}\rangle - \langle\hat{n}_{yCj}\rangle = \langle\hat{n}_{xCi}\rangle - \langle\hat{n}_{yBj}\rangle = \chi_{\rm SN}, \end{aligned} \tag{6}$$

where $\chi_{\rm QAH}$ denotes the order parameter for the *QAH* state that generates loop-current with broken time-reversal symmetry (TRS). Such state carries topologically protected chiral-edge states. The *QSH* order parameter $\chi_{\rm QSH}$ on the other hand can be thought of as two systems showing *QAH* effect with each breaking time reversal symmetry, but on the whole both systems jointly preserve TRS. Such states contain helical edge states as shown in [37]. On the other hand, the spin-nematic state (SNS) order parameter $\chi_{\rm SN}$ breaks C_4 symmetry between the blue and red sub-lattices and constitutes an anisotropic semi-metal [17]. We plot the resulting phase diagram in Fig.2(d) as a function of $\alpha = a_s/a$ and dipolar strength D for excess fermion filling $m = 1/2$. In the blue region the ground state is given by the spin-nematic, whereas in the green region the ground state is a topological insulator. Within the mean-field ansatz (6) both *QAH* and *QSH* have the same energy, although this degeneracy can be broken by including higher order exchange interactions [16]. As the energy scale of such exchange term is much lower, we neglect it in our calculations. Within mean-field theory, the temperature scale for the transition to the *QAH*/*QSH* state is given by, $T_c \sim (4J_{01}^2/\Delta)\exp[-J_{01}^2/2V_{\rm xx}\Delta] \sim 0.01E_R$ for $D = 0.29$ and $\alpha = -0.7$.

Let us now discuss the experimentally realizable cold atoms systems with the possibility of dynamically creating exotic lattices. One such choice is the Fermionic ^{6}Li species in lowest two energy states with broad Feshbach resonance for the interaction strength $\alpha = a_s/a = -0.6$. For the lattice constant $a = 500$nm results in a strong scattering length $a_s \sim -300$nm which is already achieved in Lithium mixtures in Refs. [38, 39]. For a mass-imbalanced mixture the effective scattering length is scaled and $\alpha \approx (a_s/a)(1 + m_\downarrow/2m_\uparrow)$ for the same parameters as used in the case of equal mass. Thus, if one traps ^{40}K in the weaker lattice of $V_0 = 4E_{\rm R\downarrow}$ ($\downarrow$-fermions) and ^{6}Li in the stiffer lattice of $V_1 = 30E_{\rm R\uparrow}$, then the topologically protected lattice phase for a scattering length of a_s (KLi) ≈ -80nm can be achieved. Such a strongly attractive scattering length can be experimentally achievable in the narrow Feshbach resonance for ^{40}K-^{6}Li mixture due to the tunability of the magnetic field at the milli-Gauss level [40].

In conclusion, dynamical creation of exotic lattices can open up another fascinating route for experimental studies. The proposed method is very general and can be extended to other lattice structures even in three dimensions. It does not involve additional optical components other than the ones needed for creating the parent lattice, which can lead to flexibility with respect to the optical components in experimental situation.

We acknowledge the support by the EU STREP NAMEQUAM, IP AQUTE, ERC Grant QUAGATUA, AAII-Hubbard. A. P. is supported by the International PhD Project "Physics of future quantum-based informa-

tion technologies", grant MPD/2009-3/4 from Foundation for Polish Science and by the University of Gdansk grant BW 538-5400-0981-12. A.P. also acknowledges hospitality from ICFO.

[1] M. Z. Hasan, and C. L. Kane, Rev. Mod. Phys. **82**, 3045 (2010).
[2] X.-L. Qi, and S.-C. Zhang, Rev. Mod. Phys. **83**, 1057 (2011).
[3] C. Nayak, *et. al.*, Rev. Mod. Phys. **80**, 1083 (2008).
[4] M. Lewenstein, A. Sanpera, and V. Ahufinger, Ultracold Atoms in Optical Lattices: Simulating quantum many-body systems, Oxford University Press, London, (2012).
[5] J. Struck, *et. al.*, Science **333**, 996 (2011).
[6] G.-B. Jo, *et. al.*, Phys. Rev. Lett. **108**, 045305 (2012).
[7] G. Wirth, M. Ölschläger, and A. Hemmerich, Nat. Phys. **7**, 147 (2011).
[8] F. D. M. Haldane, Phys. Rev. Lett. **61**, 2015 (1988).
[9] L. Tarruell, *et. al.*, Nature **483**, 302 (2012).
[10] M. Aidelsburger, *et. al.*, Phys. Rev. Lett. **107**, 255301 (2011).
[11] P. Hauke, *et. al.*, Phys. Rev. Lett. **109**, 145301 (2012).
[12] T. Neupert, L. Santos, C. Chamon, and C. Mudry, Phys. Rev. Lett. **106**, 236804 (2011).
[13] K. Sun, W. V. Liu, A. Hemmerich, and S. Das Sarma, Nat. Phys. **8**, 67 (2012).
[14] N. Y. Yao, *et. al.* Arxiv: 1212.4839 (2012).
[15] N. Goldman, F. Gerbier, M. Lewenstein, Arxiv: 1301.4959 (2013).
[16] S. Raghu, X.-L. Qi, C. Honerkamp, and S.-C. Zhang, Phys. Rev. Lett. **100**, 156401 (2008).
[17] K. Sun, H. Yao, E. Fradkin, and S. A. Kivelson, Phys. Rev. Lett. **103**, 046811 (2009).
[18] S. Uebelacker, and C. Honerkamp, Phys. Rev. B **84**, 205122 (2011).
[19] X.-L. Qi, Y.-S. Wu, and S.-C. Zhang, Phys. Rev. B **74**, 085308 (2006).
[20] V. Apaja, M. Hyrkäs, and M. Manninen, Phys. Rev. A **82**, 041402 (2010).
[21] N. Goldman, D. F. Urban, and D. Bercioux, Phys. Rev. A **83**, 063601 (2011).
[22] R. Micnas, J. Ranninger, and S. Robaszkiewicz, Rev. Mod. Phys. **62**, 113 (1990).
[23] A. Kuklov, N. Prokof'ev, and B. Svistunov, Phys. Rev. Lett. **92**, 030403 (2004).
[24] M. Lewenstein, L. Santos, M. A. Baranov, and H. Fehrmann, Phys. Rev. Lett. **92**, 050401 (2004).
[25] O. Dutta, *et. al.*, New J. Phys. **13**, 023019 (2011).
[26] T. Sowiński, *et. al.*, Phys. Rev. Lett. **108**, 115301 (2012)
[27] O. Dutta, T. Sowiński, and M. Lewenstein, arXiv: 1202.4158.
[28] A. Rapp, X. Deng, and L. Santos, Phys. Rev. Lett. **109**, 203005 (2012).
[29] D.-S. Lühmann, O. Jürgensen, and K. Sengstock, New J. Phys. **14**, 033021 (2012).
[30] P. R. Johnson, E. Tiesinga, J. V. Porto, and C. J. Williams, New. J. Phys. **11**, 093022 (2009).
[31] W. Kohn, Phys. Rev. **115**, 809 (1959).
[32] R Lemański, J. K. Freericks, and G. Banach, Phys. Rev. Lett. **89**, 196403 (2002).
[33] J. Dalibard, F. Gerbier, G. Juzeliūnas, and P. Öhberg, Rev. Mod. Phys. **83**, 1523 (2011).
[34] J. Struck, *et. al.*, Phys. Rev. Lett. **108**, 225304 (2012).
[35] M. Lu, N. Q. Burdick, and B. L. Lev, Phys. Rev. Lett. **108**, 215301 (2012).
[36] K. Aikawa, *et. al.*, Phys. Rev. Lett. **108**, 210401 (2012).
[37] C. Wu, B. A. Bernevig, and S.-C. Zhang, Phys. Rev. Lett. **96**, 106401 (2006).
[38] T. Bourdel, *et. al.*, Phys. Rev. Lett. **93**, 050401 (2004).
[39] M. Bartenstein, *et. al.*, Phys. Rev. Lett. **92**, 120401 (2004).
[40] C. Kohstall, *et. al.*, Nature 485, 615 (2012).